PROCEEDINGS OF SCIENCE

An Overview of Longitudinal Spin Structure Measurements from JLab

Vincent Sulkosky[*†]
Massachusetts Institute of Technology
E-mail: vasulk@jlab.org

Jefferson Lab is currently one of the facilities leading the investigation of the spin structure of the nucleon. Over the past 15 years, several high precision measurements have been completed, extending our knowledge of the polarized structure functions g_1 and g_2 down to $Q^2 = 0.02$ GeV^2. In particular, the low-Q^2 range $\left(\leq 0.1 \text{ GeV}^2\right)$ from these data allows us to make a benchmark-check of Chiral Perturbation theory (χPT). Previous results for the moments of the spin structure functions in this region have shown mixed agreement. For Γ_1, the first moment of g_1, we find good consistency between data and theory. However, we have seen a surprisingly large discrepancy with χPT calculations for the δ_{LT} spin polarizability on the neutron, which is significantly less sensitive to the Δ-resonance contribution. These proceedings will discuss the recent experimental effort at low Q^2 from Jefferson Lab, including a discussion of preliminary results on the neutron. The new results on the neutron still show a sizeable discrepancy between data and theory. However, new calculations show improved agreement with data for some observables. In addition, new proton data for g_2 is also expected to help resolve the disagreement for δ_{LT}.

The 7th International Workshop on Chiral Dynamics,
August 6 -10, 2012
Jefferson Lab, Newport News, Virginia, USA

[*]Speaker.

[†]Acknowledgments: This work is supported by the U.S. Department of Energy (DOE). The Jefferson Science Associates (JSA) operates the Thomas Jefferson National Accelerator Facility for the DOE under contract DE-AC05-84ER40150.

PoS(CD12)023

1. Introduction

The experimental technique of particle scattering has been widely used in nuclear and particle physics to unveil the internal structure of nuclei and nucleons. In particular, doubly-polarized electron scattering off of the nucleon provides a powerful tool to understand the strong interaction. Lepton scattering is an ideal and clean way to access the structure of the nucleon due to our understanding of the electromagnetic interaction, which is described by Quantum Electrodynamics (QED). In addition, polarization degrees of freedom provide stringent constraints on theory. On the other hand, the nucleon's dynamics and internal structure are governed by the strong interaction and is described by the gauge theory known as Quantum Chromodynamics (QCD). Unlike QED, QCD is generally non-perturbative except at small distance scales, i.e., in high energy reactions. In the high energy region, predictions from perturbative QCD (pQCD) have been verified by comparison with experimental results from facilities such as SLAC, CERN and DESY. However, at low energies in the domain of non-perturbative QCD, calculations become difficult due to the complicated interactions of the quarks and gluons in the nucleon. Therefore low-energy effective field theories such as Chiral Perturbation Theory (χPT) or numerical methods (Lattice QCD) have been utilized to make predictions. In these proceedings, the experimental program at Jefferson Lab (JLab) that involves testing Chiral effective theories at low four-momentum transfers squared will be discussed.

2. Inclusive Electron Scattering

In the process of inclusive lepton-nucleon scattering only the scattered lepton is detected:

$$l(p)+N(P)\rightarrow l(p')+X(P'), \tag{2.1}$$

where a charged lepton l, in our case an electron, scatters from a nucleon N. The relevant kinematic variables are the incident and scattered electron four-momenta $p^{\mu}=(E,\vec{k})$ and $p'^{\mu}=(E',\vec{k'})$ respectively and the nucleon four-momenta $P^{\mu}=(E_{\mathrm{t}},\vec{P})$. Since the target is at rest, $P^{\mu}=(M,\vec{0})$ in the laboratory system. The scattering angle is θ. The exchanged virtual photon carries four-momentum $q^{\mu}=(p-p')^{\mu}=(\nu,\vec{q})$ with energy $\nu=\frac{P\cdot q}{M}=E-E'$ and momentum $\vec{q}$ to the target. The differential cross section is a function of two Lorentz invariants and the scattering angle. Typically, the squared four-momentum transfer $\left(Q^2\right)$ and the invariant mass of the residual hadronic system (W) are used:

$$Q^2\equiv -q^2\simeq 2EE'(1-\cos\theta) \tag{2.2}$$

$$W=\sqrt{(P+q)^2}=\sqrt{M^2+2M\nu-Q^2} \tag{2.3}$$

However, the Bjorken scaling variable $x=Q^2/2M\nu$ is also used, which in the parton model represents the fraction of nucleon momentum carried by the struck quark.

The inclusive cross section for electron-nucleon scattering is proportional to the product of a leptonic and a hadronic tensor, $L_{\mu\nu}$ and $W^{\mu\nu}$, respectively. The leptonic tensor is calculable from

QED, and the hadronic tensor can be split into symmetric and antisymmetric parts. The internal structure of the nucleon is described by four structure functions: $F_{1,2}$ and $g_{1,2}$, where the structure functions $g_1\left(x,Q^2\right)$ and $g_2\left(x,Q^2\right)$ contain information on the spin structure of the nucleon.

3. Spin Structure of the Nucleon and Sum Rules

The internal structure of the nucleon is parametrized by structure functions; however, the available theoretical tools are unable to calculate them. Instead, theories are used to provide predictions of the moments of the structure functions; in these proceedings, the n-th moments are used with $\Gamma^n_{1,2} = \int_0^1 x^{n-1} g^N_{1,2}\left(x,Q^2\right) dx$, where N is either the proton or neutron. In addition to the moments, there are several dispersive sum rules that link the forward Compton scattering amplitudes to integrals of the inclusive photoproduction cross sections. Sum rules utilize dispersion relations, which relate the integral over the imaginary part of a quantity to its real part. When coupled with additional hypotheses such as a low energy theorem, the integrals can often be related to a static property of the nucleon, e.g., its anomalous magnetic moment. The static properties are typically well known, and hence, the confirmation of the sum rule provides a test of the theory and assumptions used in its derivation. Clearly, sum rules provide a useful testing ground to study the internal degrees of freedom of the system.

There are several spin dependent sum rules. However in these proceedings, we will focus on the Gerasimov-Drell-Hearn (GDH) sum rule [1], the Bjorken sum rule [2] and the forward spin polarizabilities [3, 4] at low- and intermediate-Q^2 values. Refs. [4 – 6] provide detailed reviews on the experimental and theoretical efforts in this field.

3.1 Generalized GDH and Bjorken Sum Rules

The Gerasimov-Drell-Hearn (GDH) sum rule relates a particle's anomalous magnetic moment κ to an energy-weighted integral over its photoabsorption cross section. The sum rule's significance is that it relates static properties of the particle's ground state to dynamic properties of all its excited states. It also divulges that a particle with a finite size and an excitation spectrum is required to have a non-zero anomalous magnetic moment [3]. The sum rule for spin-$\frac{1}{2}$ particles is

$$\int_{\nu_0}^{\infty} \frac{d\nu}{\nu}\left[\sigma_{\frac{1}{2}}(\nu) - \sigma_{\frac{3}{2}}(\nu)\right] = -2\pi^2\alpha\frac{\kappa^2}{M^2}\,, \tag{3.1}$$

where $\nu_0 = m_\pi\left(1+\frac{m_\pi}{2M}\right) \approx 150$ MeV is the threshold energy for pion production. The anomalous magnetic moment and mass of the target are κ and M, respectively and α is the electromagnetic coupling constant. $\sigma_{\frac{1}{2}}$ and $\sigma_{\frac{3}{2}}$ are the photoabsorption cross-sections, where the sum of the photon and target helicities in the center of mass system is 1/2 and 3/2. The GDH sum rule is also valid for any target with definite spin-S.

The GDH integral (left hand side of Eq. 3.1) was generalized [7] to virtual photon absorption $\left(Q^2 > 0\right)$ by replacing the photoabsorpton cross-sections with the electroproduction cross-sections. Additional extensions have also been proposed [3, 8]. The extension of Ji and Osborne [8] relates the integral to the forward virtual Compton scattering amplitude $S_1\left(0,Q^2\right)$ to form a Q^2-dependent sum rule:

$$\frac{8}{Q^2}\int_0^{x_0} g_1\left(x,Q^2\right) dx = S_1\left(0,Q^2\right)\,, \tag{3.2}$$

where $x_0 = \frac{Q^2}{2M\nu_0}$. This extension provides a relation that is constrained at the two ends of the Q^2 spectrum by well known sum rules: GDH at $Q^2 = 0$ and the Bjorken sum rule [2] at large Q^2.

The Bjorken sum rule relates the integral over the isovector component of the g_1 structure function $\left(g_1^p - g_1^n\right)$ to the axial charge of the nucleon, g_A. This sum rule is valid at infinite Q^2, but like the GDH sum rule, it has also been generalized to finite Q^2 via the Operator Product Expansion of pQCD:

$$\begin{aligned}\Gamma_1^{p-n}\left(Q^2\right) &\equiv \int_0^1 \left[g_1^p\left(x,Q^2\right) - g_1^n\left(x,Q^2\right)\right] dx \\ &= \frac{g_A}{6}\left[1 - \frac{\alpha_s\left(Q^2\right)}{\pi} - 3.58\frac{\alpha_s^2\left(Q^2\right)}{\pi^2} - 20.21\frac{\alpha_s^3\left(Q^2\right)}{\pi^3} + \ldots\right] + \ldots,\end{aligned} \tag{3.3}$$

where $\alpha_s\left(Q^2\right)$ is the coupling constant of the strong interaction. The expression in brackets represents the leading twist term and has a mild Q^2 dependence. There are also non-perturbative corrections known as higher twists to Eq. 3.3, which involve quark-gluon correlations. This sum rule has been pivotal in enhancing our knowledge of the nucleon spin structure, and the generalized sum rule has been measured and verified in polarized deep inelastic scattering (DIS) at CERN [9], DESY [10, 11] and SLAC [12]. Over the past decade, JLab experiments have increased the coverage at low and moderate Q^2 [13 – 19].

Clearly, there is a close relationship between the Bjorken and generalized GDH integrals:

$$I_{GDH}^{p-n}\left(Q^2\right) = \frac{Q^2}{8} \times \Gamma_1^{p-n}\left(Q^2\right). \tag{3.4}$$

The extended GDH and Bjorken sum rules can be used to make comparisons between theoretical calculations and experimental data over the entire Q^2 range. At high Q^2, the Bjorken sum rule provides the prediction, whereas at intermediate and low Q^2 Lattice QCD and χPT provide the predictions, respectively, of the spin dependent Compton amplitude in Eq. 3.2. These comparisons also allow an important investigation of the transition between the non-perturbative and the perturbative regions of QCD.

3.2 Spin Polarizabilities

Higher moments of the polarized structure functions are connected to electromagnetic polarizabilities by sum rules that characterize the coherent response of the nucleon to photon absorption. The generalized spin polarizabilities characterize the response to virtual photons. Due to the higher power of x weighting, these integrals converge faster than the first moments, and therefore are less sensitive to the unmeasured low-x contributions. The expressions for the γ_0 and δ_{LT} polarizabilites in terms of the structure functions are given by

$$\gamma_0\left(Q^2\right) = \frac{16\alpha M^2}{Q^6}\int_0^{x_0} x^2\left[g_1\left(x,Q^2\right) - \frac{4M^2}{Q^2}x^2 g_2\left(x,Q^2\right)\right] dx, \tag{3.5}$$

$$\delta_{\mathrm{LT}}\left(Q^2\right) = \frac{16\alpha M^2}{Q^6}\int_0^{x_0} x^2\left[g_1\left(x,Q^2\right) + g_2\left(x,Q^2\right)\right] dx. \tag{3.6}$$

The derivation of the sum rules for the spin polarizabilities are discussed in [4].

For the longitudinal-transverse polarizability, δ_{LT}, the Δ-resonance contribution of 1232 MeV is suppressed, since the transition is mostly transverse. Hence, based on this fact, δ_{LT} is expected to provide a robust quantity to calculate within χPT.

In the next section, results on these sum rules from the Jeffeson Lab low-Q^2 experiments will be discussed.

4. Experimental Measurements of Moments for $Q^2 \approx 0.1$ GeV^2

The results discussed below are from data taken with the JLab polarized electron beam with beam polarization near 85% and beam currents up to 15 μA, 0.01μA, 0.1 μA for experimental halls: A, B and C, respectively. Hall B has a large acceptance spectrometer [20] known as CLAS for measurements over an extensive kinematic region. Hall A [21] and C have smaller acceptance spectrometers with high luminosity for higher precision measurements.

Polarized targets have been utilized in each of the halls. In Hall A, a gaseous ^{3}He target is polarized by spin exchange optical pumping. The ground state of the ^{3}He nucleus is predominatly in the S-state, where the two proton spins are anti-aligned due to the Pauli exclusion principle. Hence, polarized ^{3}He can be utilized as an effective polarized neutron target. A high luminosity of 10^{36} s^{-1} cm^{-2} has been achieved with polarizations of beam on target over 60%. In these proceedings, the focus will be on the neutron results. However, results from ^{3}He data have also been published [18]. In Hall B and C solid targets [22] made of polarized ammonia NH_3 and ND_3 are often employed. These targets are polarized via Dynamical Nuclear Polarization. The targets have reached polarized luminosities of 10^{34} s^{-1} cm^{-2} and 10^{35} s^{-1} cm^{-2} in Hall B and C, respectively with polarizations up to 90% for the proton and to 40% for the deuterated targets. Since light nuclear targets are required to study the neutron internal structure, the extraction of neutron information from both polarized deuteron and ^{3}He provides a critical systematic check of our understanding of the nuclear effects involved. The target in Hall C has been exclusively used at moderate-Q^2 values $\left(> 1 \text{ GeV}^2\right)$, and hence, the results from these data [17] will not be discussed.

4.1 Results on the First Moment of g_1

In Figure 1, the measured results for the proton and Bjorken sum (isovector component) of the first moment of g_1 are presented. As can clearly be seen, the data cover a large range in Q^2 from 0.05 GeV^2 up to 3 GeV^2 including the region where χPT is expected to be valid. The data are gathered from experiments carried out at CERN [9], DESY [10, 11], JLab [13 – 17] and SLAC [12]. A comparison between the data and χPT calculations [23, 24] can be seen at low Q^2 in the figure. The slope at $Q^2 = 0$ is taken from the GDH sum rule, and hence, the χPT calculations provide the deviation from the slope. It is this deviation that can be checked between the experimental data and the predictions. A fit has been performed for the proton and Bjorken sum [16] with the form:

$$\Gamma_1^N = \frac{\kappa_N^2}{8M^2} Q^2 + aQ^4 + bQ^6 \,, \tag{4.1}$$

where N is either the proton or neutron. For the proton and Bjorken sum, the determined numerical values for a from experiment and theory are listed in Table 1. The fits to the data indicate

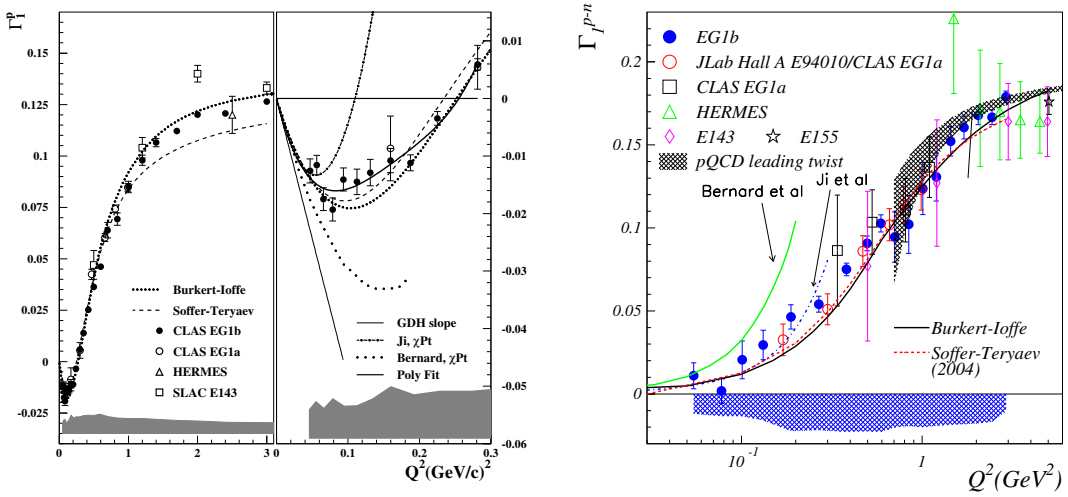

Figure 1: Experimental results from CERN, DESY, JLab and SLAC on Γ_1 for the proton (left) and isovector component (right) in the low- and moderate-Q^2 regions. The theoretical curves and models are explained in the text.

Nucleon Component	a_{exp}	$a_{\rm Ji}$	$a_{\rm BM}$
Proton	$4.31 \pm 0.31 \pm 1.36$	3.89	
P–N	$0.80 \pm 0.07 \pm 0.23$	0.74	2.4
P+N	$6.97 \pm 0.96 \pm 1.48$	7.11	

Table 1: Numerical values of a from the Q^2-dependent fit compared to χPT calculations $a_{\rm Ji}$ [23] and $a_{\rm BM}$ [24].

the importance of the Q^6 term at $Q^2 < 0.1$ GeV^2. The data and χPT calculations are in good agreement for the proton up to $Q^2 \sim 0.08$ GeV^2; however, they agree over a much larger range up to 0.3 GeV^2 for the Bjorken sum. The data also agree very well with the two phenomenological model calculations [25, 26].

4.2 Results on Spin Polarizabilities

The data from Hall A and Hall B are shown in Fig. 2 for the spin polarizabilities in the low-Q^2 region. The left panel of the figure provides the isospin decomposition of the data from both Hall A and B for the γ_0 spin polarizability with the two independent χPT calculations[24, 27] indicated on the graph. In the right panel of Fig. 2, the neutron spin polarizabilities for γ_0 and $\delta_{\rm LT}$ are shown. The light shaded band also includes the Δ-resonance and vector meson contributions for the relativistic baryon χPT (RBχPT) calculation [24]. The data are also compared to the MAID model [3, 28], which shows very good agreement with the data over most of the Q^2 range. Surprisingly, there is little agreement between the available data and χPT calculations, except perhaps for γ_0^n at the lowest-Q^2 point and the RBχPT band. The quantity $\delta_{\rm LT}$ is most puzzling, since it is mostly insensitive to the Δ-resonance contribution compared to the γ_0 polarizability. This disagreement has been referred to as the "$\delta_{\rm LT}$ puzzle" and presents a real challenge to theorists, possibly

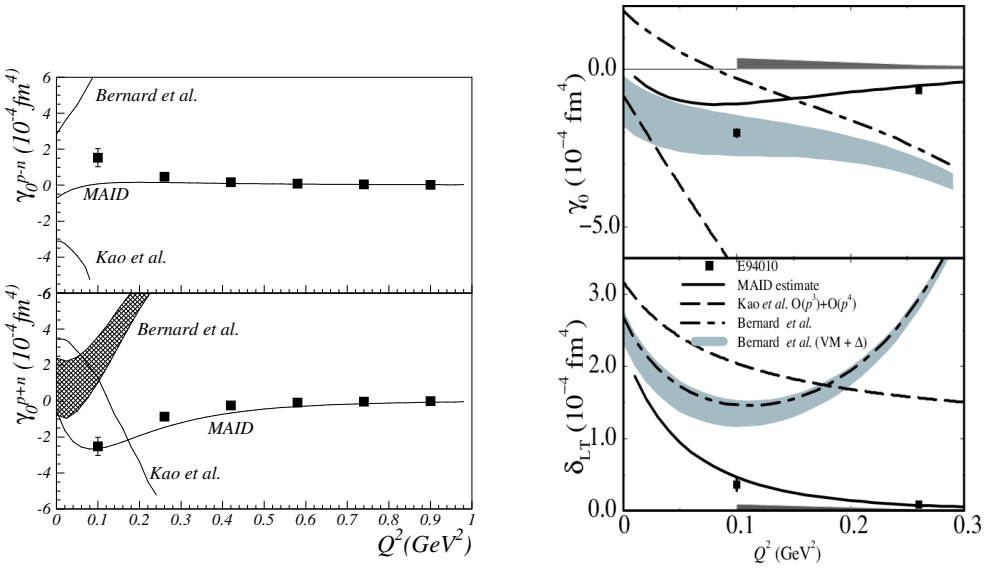

Figure 2: JLab data on the generalized spin polarizabilities at low Q^2. The isopsin decomposition of γ_0 [16] from the combined Hall A and B data [13, 14] is shown on the left-hand side $\left(\text{top}:\gamma_0^{p-n}, \text{bottom}:\gamma_0^{p+n}\right)$. The right-hand side of the figure shows the neutron spin polarizabilities γ_0 (top panel) and δ_{LT} (bottom panel) from the Hall A data.

indicating that the inclusion of the resonance contributions may not be the only issue. One of the major limitations of the available data was that the lowest Q^2 point might still be outside the region of χPT's applicability. Since these data were published, recently completed experiments at JLab have obtained data for Q^2 down to approximately 0.02 GeV^2, where the data should be well within the χPT domain of validity.

5. Recent Experimental Progress and Preliminary Results

All the data discussed so far have covered the intermediate Q^2 region. However, a new set of high precision experiments has recently been completed at JLab with an emphasis on extending the data to lower Q^2 to make a bench-mark check of χPT predictions. This section will briefly discuss new g_1 measurements on the proton and deuteron from Hall B [29] and present the preliminary Hall A results on the neutron [30] from a polarized ^{3}He target. A new measurement on the proton δ_{LT} polarizability [31] from Hall A was also presented at this conference by C. Gu and P. Zhu. The plan for all these measurements was to extend the measured-Q^2 range down to ~ 0.02 GeV^2.

The main goal of the Hall B EG4 experiment [29] was to measure the g_1 structure function for both polarized NH_3 and ND_3 targets via doubly-polarized inclusive electron scattering at low Q^2. In Hall B, the target can only be polarized along the beam direction, which mostly provides access to g_1. On the other hand, the polarized ammonia target in Hall C can be polarized in directions along the beam and perpendicular (in the horizontal plane). Hence, the spokespersons for experiment E08-027 [31] decided to move the Hall C target into Hall A to measure the g_2 structure function, which provides the data necessary to determine the δ_{LT} polarizability for the proton between 0.02 GeV^2 and 0.16 GeV^2 when combined with the Hall B g_1 data.

For the EG4 experiment, the electron beam was polarized to about 80% with beam energies of 1–3 GeV. Since the cross section difference measurements require an uniform and high detection efficiency of electrons across the spectrometer acceptance, a new Cherenkov detector was installed in the CLAS spectrometer for detection of small angle scattering down to 6°. This experiment achieved good coverage of the resonance region for $0.015 < Q^2 < 0.5$ GeV^2. Currently, the data analysis is ongoing, and preliminary cross section differences were shown during the conference.

Hall A experiment E97-110 acquired data using the JLab longitudinally polarized electron beam, which was scattered on either a longitudinally or transversely (in-plane) polarized ^{3}He target [21]. The doubly-polarized inclusive cross-section differences were measured. From these data, the polarized structure functions were extracted to form the integrals at Q^2 between 0.04 and 0.24 GeV^2. The experimental details and data analysis can be found in [30]. The experiment made a high precision measurement of the moments of the spin structure functions in a previously unmeasured region of kinematics to test χPT calculations. It also complements the data from the early Hall A experiment [14, 18].

For this experiment, the polarized ^{3}He target was used as an effective neutron target. The neutron moments were extracted from the measured ^{3}He quantities by using the technique described in [32]. The systematic uncertainty due to this extraction was determined to be 10% for $Q^2 \leq 0.1$ GeV^2 and 5% at higher Q^2. The deuteron data from EG4 will also provide an important systematic check of the neutron extraction. The parametrization in [33] was used to account for the unmeasured low-x contribution for the generalized GDH integral.

In the top graph of Fig. 3, the preliminary results for the first moment Γ_1^n, where the elastic contribution to the integral is excluded, are compared to theoretical calculations and earlier measurements [11 – 14]. The solid triangles show the preliminary data, and the inverted triangles indicate the results from a previous Hall A experiment [14]. The Hall B EG1b data are not shown for clarity. The error bars indicate the size of the total uncertainties with the statistical and systematic uncertainties added in quadrature. The data agree well with the earlier data and the two model calculations [25, 26] and indicate a smooth transition as $Q^2 \to 0$. Two calculations from χPT are also shown on the figure; the calculation with an estimate of the Δ-resonance and vector meson contributions is represented by the shaded band. With the current uncertainties, the data show good agreement with the RBχPT calculation [24], and the three lowest-Q^2 points also agree well with the heavy baryon χPT (HBχPT) calculation [23].

The γ_0 and $\delta_{\rm LT}$ polarizabilities for the neutron appear in the bottom-left and bottom-right panels of Fig. 3, respectively. The solid circles show the preliminary data, and the squares indicate the results from a previous Hall A experiment [14] between 0.1 GeV^2 and 0.26 GeV^2. The error bars on the data indicate the size of the statistical uncertainties, and the solid bands near zero show the size of the systematic uncertainties. The band on the negative side of the vertical axis is for the new data. The γ_0 data agree reasonably well with the earlier data and the MAID model [3, 28]. For $\delta_{\rm LT}$, the data and the model agree extremely well with each other. The two available calculations from χPT [24, 27] are also shown in the graphs. The light-shaded band represents the calculation with an estimate of the Δ-resonance and vector meson contributions. Within the current uncertainties, the γ_0 results show good agreement with the RBχPT calculation below 0.12 GeV^2. However, the HBχPT [27] calculation shows a large discrepancy, which might indicate the importance of the resonances for this observable. Preliminary results for the $\delta_{\rm LT}$ polarizability show good agreement

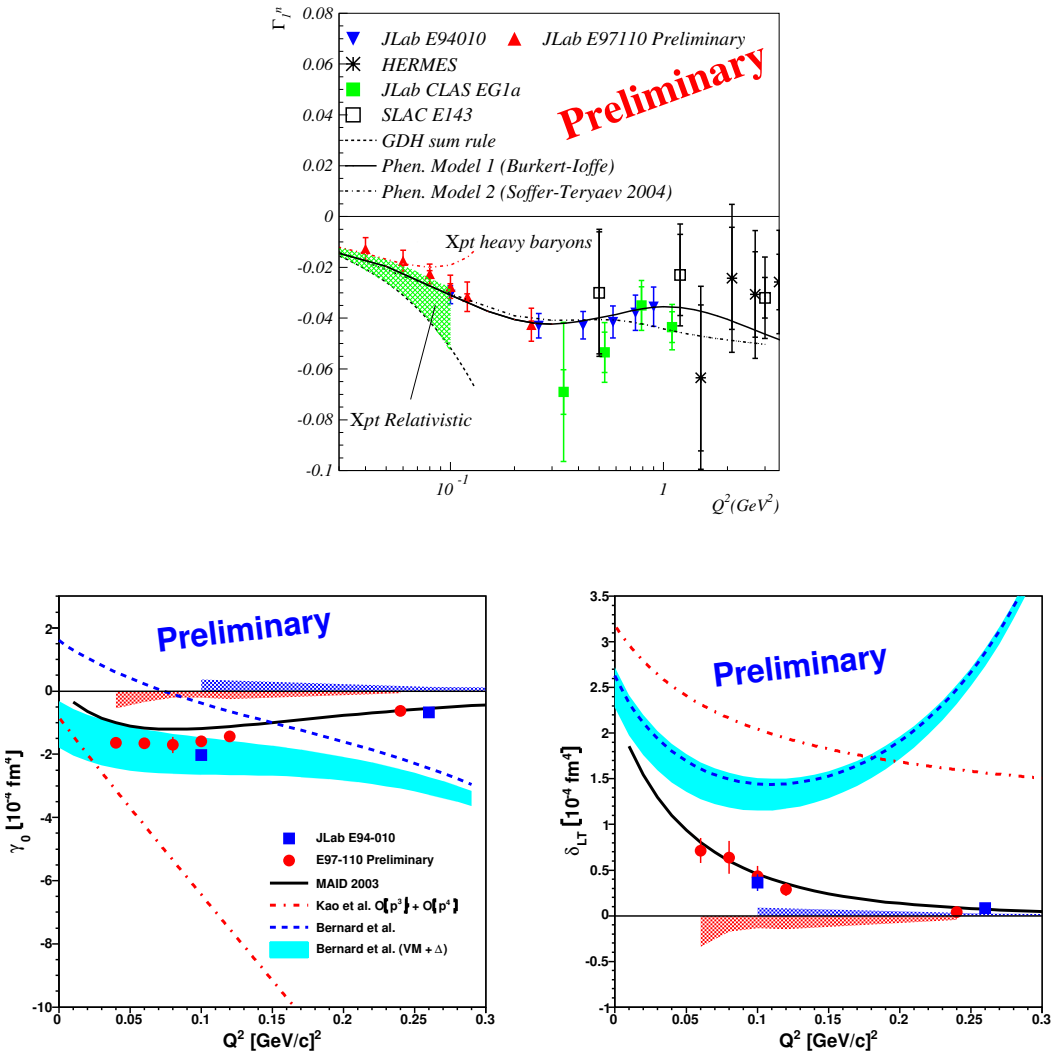

Figure 3: Preliminary neutron Γ_1^n (top panel), γ_0^n (bottom-left panel) and δ_{LT} (bottom-right panel) results. The theoretical curves and models are explained in the text.

with the previously published data and a very significant discrepancy with the χPT calculations. However, recent theoretical progress [34] has been made is that is not yet reflected in these graphs. For these preliminary data, we are in the process of significantly improving the largely dominant systematic uncertainties for the final results.

6. Summary

In these proceedings, we have discussed the data from Jefferson Lab experiments on the moments of the spin-dependent structure functions for the proton and neutron at low-Q^2 values, where χPT calculations are expected to be valid. In general, the comparison between the data and calculations have mixed agreement with the best agreement occurring for the Bjorken sum and for the

generalized GDH sum. For observables in which the Δ-resonance contribution is highly suppressed such as δ_{LT}^{n}, the discrepancy is rather significant and unexpected. Recent experimental endeavors have acquired data at lower Q^2 and on a transversely polarized proton target, providing data for δ_{LT}^{p}, which might help resolve the disagreement between experiment and theory. Progress has also been made in theory calculations that appears to be bridging the gap between the data and earlier predictions.

References

[1] S. B. Gerasimov, *Sov. J. Nucl. Phys.* **2** (1966) 430;
S. D. Drell and A. C. Hearn, *Phys. Rev. Lett.* **16** (1966) 908.

[2] J. D. Bjorken, *Phys. Rev.* **148** (1966) 1467; *Phys. Rev.* D **1** (1970) 465; *Phys. Rev. D* **1** (1970) 1376.

[3] D. Drechsel, S. S. Kamalov and L. Tiator, *Phys. Rev. D* **63** (2001) 114010 [hep-ph/0008306];
D. Drechsel, B. Pasquini and M. Vanderhaeghen, *Phys. Rept.* **378** (2003) 99 [hep-ph/0212124].

[4] J.-P. Chen, A. Deur and Z.-E. Meziani, *Mod. Phys. Lett. A* **20** (2005) 2745 [nucl-ex/0509007].

[5] S. E. Kuhn, J.-P. Chen and E. Leader, *Prog. Part. Nucl. Phys.* **63** (2009) 1 [hep-ph/08123535].

[6] J.-P. Chen, *Int. J. Mod. Phys. E* **19** (2010) 1893 [nucl-ex/10013898]

[7] M. Anselmino, B. L. Ioffe and E. Leader, *Sov. J. Nucl. Phys.* **49** (1989) 136.

[8] X. Ji and J. Osborne, *J. Phys. G* **27** (2001) 127 [hep-ph/9905410].

[9] D. Adeva *et al.*, *Phys. Rev. D* **58** (1998) 112001.

[10] K. Ackerstaff *et al.*, *Phys. Lett. B* **404** (1997) 383; *Phys. Lett. B* **444** (1998) 531.

[11] A. Airapetian *et al.*, *Phys. Lett. B* **442** (1998) 484; *Phys. Rev. Lett.* **90** (2003) 092002; *Eur. Phys. J. C* **26** (2003) 527; *Phys. Rev. D* **75** (2007) 012007.

[12] P. L. Anthony *et al.*, **54** (1996) 6620 [hep-ex/9610007]; *Phys. Lett. B* **553** (2003) 18 [hep-ex/0204028]
K. Abe *et al.*, *Phys. Rev. D* **58** (1998) 112003 [hep-ph/9802357]; *Phys. Rev. Lett.* **79** (1997) 26 [hep-ex/9705012].

[13] R. Fatemi *et al.*, *Phys. Rev. Lett.* **91** (2003) 222002 [nucl-ex/0306019];
J. Yun *et al.*, *Phys. Rev. C* **67** (2003) 055204 [hep-ex/0212044];
K.V. Dharmawardane *et al.*, *Phys. Lett. B* **641** (2006) 11 [nucl-ex/0605028];
Y. Prok *et al.*, *Phys. Lett. B* **672** (2009) 12 [nucl-ex/08022232].

[14] M. Amarian *et al.*, *Phys. Rev. Lett.* **89** (2002) 242301 [nucl-ex/0205020]; *Phys. Rev. Lett.* **92** (2004) 022301 [hep-ex/0310003]; *Phys. Rev. Lett.* **93** (2004) 152301 [nucl-ex/0406005].

[15] A. Deur *et al.*, *Phys. Rev. Lett.* **93** (2004) 212001-1.

[16] A. Deur *et al.*, *Phys. Rev. D* **78** (2008) 032001 [nucl-ex/08023198].

[17] F. R. Wesselmann *et al.*, *Phys. Rev. Lett.* **98** (2007) 132003.

[18] K. Slifer *et al.*, *Phys. Rev. Lett.* **101** (2008) 022303 [nucl-ex/08032267].

[19] P. Solvignon *et al.*, *Phys. Rev. Lett.* **101** (2008) 182502 [nucl-ex/08033845].

[20] B. Mecking *et al.*, *Nucl. Instrum. and Meth. A* **503** (2003) 513.

[21] J. Alcorn *et al.*, *Nucl. Instrum. Meth. A* **522** (2004) 294.

[22] C. D. Keith *et al.*, *Nucl. Instrum. Meth. A* **501** (2003) 327.

[23] X. Ji, C. Kao and J. Osborne, *Phys. Lett. B* **472** (2000) 1 [hep-ph/9910256].

[24] V. Bernard, T. R. Hemmert and U.-G. Meissner, *Phys. Lett. B* **545** (2002) 105 [hep-ph/0203167]; *Phys. Rev. D* **67** (2003) 076008 [hep-ph/0212033].

[25] V. D. Burkert and B. L. Ioffe, *Phys. Lett. B* **296** (1992) 223.

[26] J. Soffer and O. V. Teryaev, *Phys. Rev. D* **70** (2004) 116004 [hep-ph/0410228].

[27] C. W. Kao, T. Spitzenberg and M. Vanderhaeghen, *Phys. Rev. D* **67** (2003) 016001 [hep-ph/0209241].

[28] D. Drechsel, O. Hanstein, S. S. Kamalov, and L. Tiator, *Nucl. Phys. A* **645** (1999) 145.

[29] M. Battaglieri, A. Deur, R. De Vita and M. Ripani, JLab experiment E03-006.

[30] V. Sulkosky, *The Spin Structure of ^{3}He and the Neutron at Low Q^2: A Measurement of the Generalized GDH Integrand*, http://hallaweb.jlab.org/experiment/E97-110/thesis.html.

[31] A. Camsonne, J. P. Chen and K. Slifer, JLab experiment E08-027.

[32] C. Ciofi degli Atti and S. Scopetta, *Phys. Lett. B* **404** (1997) 223 [nucl-th/9606034].

[33] N. Bianchi and E. Thomas, Phys. Lett. **B450** 439 (1999); *Nucl. Phys. Proc. Suppl.* **82** (2000) 256.

[34] V. Bernard, E. Epelbaum, H. Krebs and U.-G. Meissner, (2012) [hep-ph/12092523].